Journal of Materials Chemistry B

Enhanced Multi-Lineage Differentiation of Human Mesenchymal Stem/Stromal Cells within Poly (N-isopropylacrylamide-Acrylic Acid) Microgel-Formed Three-Dimensional Constructs

Journal:	*Journal of Materials Chemistry B*
Manuscript ID	TB-ART-02-2018-000376.R1
Article Type:	Paper
Date Submitted by the Author:	28-Feb-2018

Complete List of Authors:	Zhang, Jiabin; University of Adelaide Faculty of Engineering Computer and Mathematical Sciences, School of Chemical Engineering Yun, Seonho; University of Adelaide Faculty of Engineering Computer and Mathematical Sciences, School of Chemical Engineering Bi, Jingxiu; The University of Adelaide, School of Chemical Engineering Dai, Sheng; University of Adelaide Faculty of Engineering Computer and Mathematical Sciences, School of Chemical Engineering Du, Yuguang ; Key Laboratory of Biopharmaceutical Production & Formulation Engineering, PLA and State Key Laboratory of Biochemical Engineering, Institute of Process Engineering, Chinese Academy of Sciences Zannettino, Andrew; University of Adelaide, Zhang, Hu; The University of Adelaide, School of Chemical Engineering

Enhanced Multi-Lineage Differentiation of Human Mesenchymal Stem/Stromal Cells within Poly (N-isopropylacrylamide-Acrylic Acid) Microgel-Formed Three-Dimensional Constructs

Jiabin Zhang[1], Seonho Yun[1], Jingxiu Bi[1], Sheng Dai[1], Yuguang Du[3], Andrew C.W. Zannettino[2], Hu Zhang[1]**

[1]School of Chemical Engineering, The University of Adelaide, Adelaide, SA 5005, Australia
[2]Adelaide Medical School, The University of Adelaide, Adelaide, SA 5001, Australia
[3]Institute of Process Engineering, Chinese Academy of Sciences, Beijing, 100190, China
[*]Corresponding author: E-mail: hu.zhang@adelaide.edu.au (H.Z.), E-mail: andrew.zannettino@adelaide.edu.au (A.C.W.Z.)

Abstract

Human mesenchymal stem/stromal cells (hMSCs) are a potential cell source of stem cell therapy for many serious diseases and hMSC spheroids have emerged to replace single cell suspensions for cell therapy. Three dimensional (3D) scaffolds or hydrogels which can mimic properties of the extracellular matrix (ECM) have been widely explored for their application in tissue regeneration. However, there are considerably less studies on inducing differentiation of hMSC spheroids using 3D scaffolds or hydrogels. This study is the first to explore multi-lineage differentiation of a stem cell line and primary stem cells within poly (N-isopropylacrylamide) (p(NIPAAm))-based thermosensitive microgel-formed constructs. We first demonstrated that poly (N-isopropylacrylamide-co-acrylic acid) (p(NIPAAm-AA)) was not toxic to hMSCs and the microgel-formed constructs facilitated formation of uniform stem cell spheroids. Due to functional enhancement of cell spheroids, hMSCs within the 3D microgel-formed constructs were induced for multi-lineage differentiation as evidenced by significant up-regulation of messenger RNA (mRNA) expression of chondrogenic and osteogenic genes even in the absence of induction media on day 9. When induction media were in-situ supplied on day 9, mRNA expression of chondrogenic, osteogenic and adipogenic genes within the microgel-formed construct were significantly higher than that in the pellet and 2D cultures, respectively, on day 37. In addition, histological and immunofluorescent images also confirmed successful multi-lineage differentiation of hMSCs within the 3D microgel-formed constructs. Hence, the thermosensitive p(NIPAAm-AA) microgel can be potentially used in an *in-vitro* model for cell differentiation or *in-vivo* transplantation of pre-differentiated human mesenchymal stromal cells into patients for specific lineage differentiation.

Keywords: poly (N-isopropylacrylamide); microgel; multi-lineage differentiation; tissue engineering; cell spheroid; human mesenchymal stem/stromal cell

Introduction

Stem cells, such as human mesenchymal stromal cells (hMSCs), are a potential cellular therapy source to treat serious diseases [1], such as cartilage injury [2-4], spinal injury [5, 6] and cardiac failure [7-9]. They can be differentiated into chondrocytes [10, 11], osteoblasts [12, 13] and adipocytes [14] both *in vitro* and *in vivo*. [15] However, the lack of cell retention within the defective sites following injection as single-cell suspensions limits their clinical application. [16] Hence, stem cell spheroids are emerging as an alternative to single cell suspension to improve cell retention during implantation. [16, 17] Recent reports also suggest that hMSC spheroids possess enhanced anti-inflammatory and multi-lineage differentiation properties. [16, 18, 19]

However, cellular spheroids have to be carefully prepared for clinical application to mitigate issues, such as necrosis within the center of the spheroid [20]. The size of cellular spheroids is one of important parameters for quality control. It is also essential to have a better understanding of differentiation of cellular spheroids *in vitro* so that the spheroids can be applied to patients.

Three-dimensional (3D) microenvironments are known as native niches that can significantly regulate migration, proliferation, and differentiation of stem cells. [21, 22] The extracellular matrix (ECM) of tissues provides both physical and biochemical cues, such as stiffness and RGD-motifs, respectively, which act in concert to influence cell behavior. [23-25] Water-rich smart hydrogels, allowing mimicking the properties of ECM and customized incorporation of other biochemical stimuli, recently become attractive for stem cell-based tissue engineering. [11, 26-30] Thermosensitive hydrogels are one example of smart hydrogels that can respond to temperature change. They are highly porous and abundant in water, providing 3D mechanical support for cells and facilitating gas and mass exchange between the incorporated cells and the surrounding environment. [31]

Poly (N-isopropylacrylamide) (p(NIPAAm)) is a widely used thermosensitive polymer that can reversibly transform from sol to gel status when heated above its lower critical solution temperature (LCST), 32 °C, which is close to the temperature of human body. [32] It can be easily synthesized in a large quantity and even bonded with natural components, such as RGD peptides [33], gelatin [34], hyaluronic acid [14], chitosan [35], to improve its biological properties. When a pNIPAAm hydrogel forms a gel, water is expelled out of the hydrogel and the hydrogel shrinks, via a process of syneresis, making it unsuitable for cell culture. To prevent the syneresis, hydrophilic components, such as acrylic acid (AA), are copolymerized with pNIPAAm. In addition, after further crosslinking, thermosensitive p(NIPAAm-AA) microgels are produced. [32] Once the carboxyl groups of p(NIPAAm-AA) are ionized, the p(NIPAAm-AA) microgel has a negative charge and makes the internal porosity larger, allowing more efficient gas and mass exchange. [32]

Stem cell differentiation into single type of cells in the thermosensitive hydrogels has been reported and the 3D microenvironment offered from the hydrogels is found to have a great impact on cellular differentiation. [35-39] However, there are very few studies comprehensively examining the multi-lineage differentiation of human mesenchymal stromal cell spheroids generated within p(NIPAAm)-based thermosensitive microgel-formed constructs. [15, 16] Therefore, in this study, we successfully synthesized a thermosensitive p(NIPAAm-AA) microgel that not only mimicked 3D ECM properties but also facilitated spheroids harvest because of its thermal reversibility. The microgel showed no toxicity to the hMSCs from both 2D and 3D toxicity assays. After they were cultured within the 3D microgel-formed construct, hMSCs formed uniform cell spheroids of 100 μm in diameter without central necrosis [20], while they proliferated at a much slower rate than the hMSCs grown in 2D conventional culture. Messenger RNA (mRNA) expression of chondrogenic, osteogenic and adipogenic genes were significantly upregulated for both immortalized bone marrow derived

human mesenchymal stem/stromal cells (UE7T-13) and primary normal donor derived human mesenchymal stem/stromal cells (NOD MSCs) in microgel-formed 3D constructs than that in pellet and 2D cultures, respectively. Even in the absence of induction media, UE7T-13 displayed multi-lineage differentiation with a relatively higher mRNA expression of chondrogenic genes (SOX9 and aggrecan) and osteogenic genes (RUNX2 and osterix) due to inductive properties of the matrix and the formation of cell spheroids [16]. Histological images revealed rich glycosaminoglycan (GAGs) distributing within complex chondrogenic micro-tissues, calcification within osteogenic cells, and lipids within adipogenic cells. Immunofluorescent images also showed distinct collagen II A1, osteocalcin and perilipin signals. Hence, we can conclude that the thermosensitive microgel-formed constructs can effectively induce multi-lineage differentiation of human stem cells, which can be potentially used in an *in-vitro* model for cell differentiation and tissue engineering or *in-vivo* transplantation of pre-differentiated human stem cells [40] into patients for specific lineage differentiation.

Materials and Methods

Microgel synthesis

The poly (N-isopropylacrylamide-co-acrylic acid) (p(NIPAAm-AA)) microgel was synthesized by free radical emulsion polymerization as previously described. [32] Briefly, 9.9 mmol of N-Isopropylacrylamide (NIPAAm, >98%, Tokyo Chemical Industry) (recrystallized in n-hexane and dried overnight), 0.2 mmol of N, N-methylenebisacrylamide (MBA, >99%, Sigma-Aldrich), 0.12 mmol of sodium dodecyl sulfate (SDS, >99%, BDH Laboratory Supplies Poole), and 0.1 mmol acrylic acid (AA, 99.5%, Acros Organics) were dissolved in 97 mL of Milli-Q® water. The solution was mechanically stirred and continuously degassed with nitrogen supply at 70 °C for 45 min in a 250 mL of three-necked flask. Subsequently, 3 mL of 1 mM potassium persulfate (KPS, >98%, Chem-Supply) in Milli-Q® water was injected to initiate the polymerization. After synthesis overnight, the microgel was left cool at room temperature and dialyzed with a Spectra/Por® molecular porous membrane tubing (Spectrum Labs, cut-off MW 12-14 kDa) against Milli-Q® water for one week with daily water change. The purified microgel was concentrated by heating at 70 °C, after which 100 μL of microgel was dried and weighted to calculate the final concentration.

Size distribution measurement of p(NIPAAm-AA) microgel

0.5 mg/mL of p(NIPAAm-AA) dissolved in water and 1× Dulbecco's phosphate buffered saline (DPBS, pH ≈ 7.4) were prepared, respectively. Their hydrodynamic diameters were measured by dynamic light scattering (DLS) at 25°C and 37 °C with a Zetasizer (Malvern, Nano-ZS). The detection angle was set at 90° and the intensity autocorrelation function was analyzed by the CONTIN software.

Dynamic moduli measurement

30 mg/mL p(NIPAAm-AA) microgel-formed three-dimensional (3D) constructs were prepared by mixing 50 mg/mL microgel, 0.05 M $MgCl_2$ in 1× Dulbecco's phosphate buffered

saline (DPBS, pH ≈ 7.4) and complete growth medium at a volumetric ratio of 3:1:1. The temperature was kept at 37 °C for 60 min prior to measurement by a SR 5 environmental system connected to a water bath (Julabo) and the gap was set to 0.65 mm. The elastic modulus (G') and viscous modulus (G") of the constructs were measured at different stress from 0.1 to 100 Pa under a constant frequency of 0.1 Hz by a SR5 rheometer (Rheometric Scientific) equipped with a 40 mm parallel plate geometry.

Transmittance measurement in the p(NIPAAm-AA) formed 3D constructs

P(NIPAAm-AA) formed 3D constructs were prepared in the same way as described in "Dynamic moduli measurement" section at room temperature. 100 μL of the construct was transferred into each 96-well plate in triplicates and the transmittance was read by a Molecular Devices VersaMax microplate reader. The wavelength of the light was set at 720 nm. The temperature was kept at 37 °C from 0 to 30 min. The transmittance of p(NIPAAm-AA) microgel-formed constructs were recorded every minute during heating at 37 °C. Then the p(NIPAAm-AA) microgel-formed constructs were kept at 37 °C in an incubator. After the temperature in the microplate reader was set at 25 °C, the p(NIPAAm-AA) microgel-formed constructs were transferred back to the microplate reader. The transmittance of the p(NIPAAm-AA) microgel-formed constructs was measured during cooling at 25 °C and recorded every minute for another 30 min. The transmittance in the blank wells was used as the control. The recorded data were averaged and normalized to the control.

Preparation of cell-gel 3D constructs

Briefly, microgel was sterilized by exposure to UV for 40 min. An immortalised human mesenchymal stromal cell line, UE7T-13 (RIKEN BioResources Center, Ibaraki, Japan, http://en.brc.riken.jp), or bone-derived mesenchymal stromal cells obtained from the iliac crest chips of normal donors (NOD MSCs) with an approval, RAH Protocol No.940911a, from the Royal Adelaide Hospital Ethics Committee as described previously [41, 42] (ND0127

NODs, ND0303 NODs, ND0055 NODs, ND0302 NODs, ND0057 NODs and ND0059 NODs) were cultured on T-75 flask in a humidified, 5% CO_2 and 37°C incubator with a complete growth medium feeding every other day (α-modified Eagle's medium (MEM, Sigma-Aldrich) supplemented with 10% fetal calf serum (FCS, Sigma-Aldrich) and 1× additive's (ADDs) (50 U/mL- 50 μg/mL penicillin-streptomycin (CSL), 2 mM L-glutamine (JRH), 1 mM sodium pyruvate (Sigma-Aldrich), 15 mM HEPES (Life Technologies)). Single-cell suspensions were prepared by washing twice with 1× Dulbecco's phosphate-buffered saline (DPBS, Sigma-Aldrich), trypsin digestion (GIBCO), enzyme quenching with the complete medium, discarding supernatant after centrifuging, and resuspending cells in the complete medium. The cell-gel hybrid was prepared by homogeneously mixing single-cell suspension, filter-sterilized magnesium chloride ($MgCl_2$) solution (dissolving hexahydrate magnesium chloride (Chem-Supply) in 1× DPBS and filtered with 0.22 μm of porosity of syringe filter), and the microgel at a volumetric ratio 1:1:3, resulting in the certain cell density and final concentration of 0.01M $MgCl_2$ and 30 mg/mL microgel, respectively. Passage 45-48 of UE7T-13 and passage 5-6 of NOD MSCs were used in the experiments reported.

Cell proliferation assay

Cell proliferation within the microgel was measured by 4-[3-(4-Iodophenyl)-2-(4-nitrophenyl)-2H-5-tetrazolio]-1,3-benzene disulfonate (WST-1, Sigma-Aldrich) cell proliferation assay. Briefly, 50 μL of coating microgel at a volumetric ratio of 50 mg/mL microgel : 0.05 M $MgCl_2$ in 1× DPBS : complete growth medium of 3:1:1 was coated on the each well of 96-well plate at 37 °C for 30 min. Then 125 μL of UE7T-13 cell solution with a density of 1.0×10^6 or 1.0×10^5 cells/mL was gelled on the coated 96-well plate in the humidified incubator containing 5% CO_2 at 37 °C for additional 30 min. Warm complete growth medium (125 μL) was added into each well and regularly changed every other day on

a dry block heater (Ratek Instruments) at 37 ℃ for up to 14 days. After 1, 5, 9 and 14 days, the 96-well was cooled down at room temperature and homogeneously mixed with 20 μL of WST-1 after discarding the 100 μL of complete growth medium above the hydrogel. Continuous incubation of the WST-1 mixture was carried out in a humidified incubator containing 5% CO_2 at 37 ℃ for 4 hr. The absorbed wavelength of solubilized formazan was measured at 450 nm by an iMark™ microplate reader (BIO-RAD) after liquidation of cell-gel hybrids on the ice. Cells cultured on the two-dimensional (2D) 96-well plate were considered as a control and processed in the same way as for the 3D cultures while using Milli-Q® water to replace the microgel. To eliminate the background absorbance, the same experiment was performed without cells as a reference. The difference in measured values between absorbance and reference were used for temporal profile of cell proliferation. Three different NOD MSCs (ND0302 NODs, ND0127 NODs and ND0059 NODs) with a density of 1.0×10^5 cells/mL were processed in the same way as UE7T-13.

Cell viability assay

The cytotoxicity of the microgel was measured by the MTT assay as described previously.[32] Briefly, 100 μL of UE7T-13 cells in the complete growth medium were seeded onto each well of 96-well plate at a density of 1.0×10^5 cells/mL and cell attachment was achieved by overnight incubation in a humidified incubator containing 5% CO_2 at 37 ℃. The media were changed with a series of different microgel concentration dissolved in the complete growth medium (0.05 mg/mL, 0.1 mg/mL, 0.5 mg/mL, 1 mg/mL, 5 mg/mL, 30 mg/mL) at 100 μL per well and cultured for another 24 hr. Subsequently, the medium containing the microgel was changed with the same volume of fresh complete growth medium and 10 μL of 5 mg/mL 3-(4,5-Dimethylthiazol-2-yl)-2,5-diphenyltetrazolium bromide (MTT, Thermo Fisher Scientific) was added into each well. Following an additional 4 hr incubation, all media were collected and discarded and 100 μL of dimethyl sulfoxide (DMSO, Chem-Supply) was added

to each well to dissolve the formed formazan crystals within the cells. Cells fed by the medium without the microgel were used as a control and processed in the same way as the cells exposed to the microgel. The absorbance of the dissolved formazan in DMSO was read by an iMark^{TM} microplate reader (BIO-RAD) at a wavelength of 595 nm. All reading absorbance were normalized to the absorbance value of the control and presented as relative absorbance.

Cell viability staining

UE7T-13 viability within the microgel was measured by fluorescently staining cells with the Live&Dead staining kit (Thermo Fisher Scientific). Briefly, 250 μL of coating microgel was added into each well of 48-well plate and incubated at 37°C for 30 min to initiate gel formation. The warm cell-gel hybrid with a density of 1.0×10^6 cells/mL was gently added into each microgel-coated 48-well plate that was kept at 37 °C using a hotplate. Gel formation was initiated and cells in the gel were continuously incubated in a humidified incubator containing 5% CO_2 at 37 °C with 500 μL of complete medium which was regularly changed every other day up to 9 days. The working solution was prepared as 4 μM calcein AM and 2 μM ethidium homodimer-1 in 1× DPBS. After 1 or 9 days, 500 μL of the feeding medium on each cell-gel hybrid was discarded, while the 48-well plate was cooled down at room temperature. 250 μL of the working solution was added into each well and homogeneously mixed with the cell-gel hybrid. After incubation at room temperature for 20 min, cells were imaged with a fluorescent microscope. Cell-gel hybrids on the 48-well plate without the microgel were also stained and imaged as described above. In addition, pellets (**Control 1**) were cultured by spinning down the same amount of the cells in a 10 mL polypropylene tube (SARSTEDT Australia). In addition, cells were also cultured on the 1.5% agar coated 48-well plate (**Control 2**). **Control 1** and **Control 2** were both cultured in a humidified incubator containing 5% CO_2 at 37 °C for up to 9 days with medium change

every other day. After 1 or 9 days, **Control 1** were stained as cell-gel hybrids and transferred to 48-well plate for fluorescent imaging, while **Control 2** were directly *in-situ* fluorescently imaged after Live&Dead staining with a CKX41 fluorescent microscope (Olympus). Live cells were shown as green, while dead cells were shown as red.

Trypan blue cell counting and Annexin/7-AAD apoptosis flow cytometry

UE7T-13 cell-gel hybrids were prepared on the microgel-coated 48-well plate as described in the "Cell viability staining" section. After incubation in a humidified atmosphere containing 5% CO_2 at 37 °C for 24 hr, cell-gel hybrids were liquefied at room temperature, transferred into 15 mL of polypropylene tubes and diluted with 10 mL of 1× DPBS. The cells were centrifuged at 383 rcf for 10 min and homogeneously resuspended in 500 μL fresh complete growth medium after discarding the supernatant. 11 μL of cell solution was mixed with the same volume of trypan blue (Sigma-Aldrich) and completely mixed before manual cell counting on a BS.748 cell counting chamber plate (Hawksley) under a CX41optical microscope (Olympus). Live cells without blue staining, and blue stained dead cells were counted. Cells cultured on the 2D 48-plate were used as a control and processed similarly as 3D cells. Subsequently, the number of live cells divided by the total cells was presented as cell viability. Relative cell viability was normalized with respect to the cell viability in 2D culture.

After trypan blue cell counting, the remaining cell suspensions of 3D and 2D were centrifuged in FACS tubes at 383 rcf for 2 min. The supernatant was discarded, and the cells were washed with 2 mL of cold binding buffer (10 mM HEPES and 5 mM calcium chloride (Scharlau) in 20 mL 1× Hank's balanced salt solution (Sigma-Aldrich)) and centrifuged at 383 rcf for 2 min. After the supernatant was discarded, cells were enzymatically digested in 1 mL of proteinase (1.5 mg/mL of collagenase (Scimar) and 2 mg/mL of dispase (Invitrogen)) for 10 min and neutralized in 10 mL of complete growth medium. Then cells were

centrifuged again and gently resuspended in 50 μL of binding buffer. The fresh UE7T-13 detached by enzymatic digestion from T-75 flask were centrifuged in FACS tubes and cell apoptosis induced by resuspending them in 1 mL of 100% DMSO for 10 min at room temperature (**positive control 1**) or cell necrosis by resuspending in 1 mL of 80% ethanol for 10 min on the ice (**positive control 2**). In addition, the freshly detached cells were also resuspended in 1 mL of complete growth medium (**negative control**). Then 3 mL of complete medium was added into each FACS tube of all controls. The cells were centrifuged at 383 rcf for 2 min, washed once with 2 mL of binding buffer, and resuspended in 50 μL of in-house binding buffer. 5 μL of 2.5 μg/mL PE-AnnexinV (Biolegend) and 20 μL of 7-AAD (Beckman Coulter) were added into each cell suspension of 2D or 3D. **Positive control 1** groups were stained with 5 μL of AnnexinV and 20 μL of in-house binding buffer, while **positive control 2** groups were stained with 5 μL of in-house binding buffer and 20 μL of 7-AAD. **Negative control** groups left unstained and 25 μL of in-house binding buffer was added. FACS tubes were kept in the dark and on ice for 20 min during staining. Cell apoptosis was immediately measured by a flow cytometer (BD, FACSCanto II Analyser) after 200 μL of in-house binding buffer was added into each FACS tube. Only those events which were negative to AnnexinV and 7-AAD were considered as live cells. Eventually, data was presented as relative cell viability by normalizing the percentage of live cells to those cells cultured in 2D.

Scanning electron microscopy (SEM) imaging of cell-gel 3D constructs

The UE7T-13 cell-gel hybrids were prepared as described in "Cell viability staining" section and cultured with the complete growth medium in a humidified atmosphere containing 5% CO_2 at 37 °C. After cultured overnight, the feeding medium on the top of the cell-gel hybrid was removed and cell-gel 3D constructs were immediately frozen in liquid nitrogen. The frozen cell-gel constructs were then dried under vacuum by a Christ Alpha 2-4

LD freeze dryer. The cross-sections of the cell-gel constructs were then coated with a layer of platinum and imaged with a Philips XL30 FEGSEM at an accelerating voltage of 10 kV.

STRO-1 flow cytometry

UE7T-13 cultured on 2D plates and in cell-gel constructs were prepared, respectively, in triplicate (1 unstained control + 1 STRO-1 negative control+ 1 STRO-1 positive test) as described in "Cell viability staining" section. After overnight, the cells were harvested and suspended in 1mL 1× DPBS. Then the cells were blocked with 1 mL 1× blocking buffer (Hank's balanced salt solution (Sigma-Aldrich) contained 5% heat-inactivated normal human serum, 1% bovine serum albumin (BSA, Sigma-Aldrich), 50 U/mL-50 μg/mL penicillin-streptomycin (CSL) and 5% fetal calf serum (FCS, Sigma-Aldrich)) on ice for 20 min to reduce the non-specific immunofluorescent staining. Then the supernatant was removed after spinning down cells. The cells as the unstained control were resuspended in 100 μL blocking buffer, while the cells as STRO-1 negative control and STRO-1 positive test were incubated in 100 μL 1 A6.12 (isotype matched IgM negative control/ anti-salmonella provided by Dr L Ashman) and 100 μL STRO-1 hybridoma supernatant on ice for 45 min, respectively. All cells were washed in 1 mL of washing buffer (1× Hank's balanced salt solution contained 5% FCS (Sigma-Aldrich)) and centrifuged to remove the supernatant. Then the cells as STRO-1 negative controls and STRO-1 positive tests were incubated in 100 μL 20 μg/mL of a goat-anti-mouse IgM-FITC conjugated second antibody (Southern Biotech), while the cells as unstained controls were resuspended in 100 μL washing buffer. The cells were washed in 1 mL of washing buffer after incubated on ice in the dark for 30 min and fixed in 2% paraformaldehyde (Sigma-Aldrich). The cell suspensions were then measured by a flow cytometer (BD, FACSCanto II Analyser). The representatives of STRO-1 flow cytometry for UE7T-13 cells cultured on 2D plates and in microgel-formed 3D constructs were then presented.

Cell cycle assay

UE7T-13 cell-gel constructs were prepared in triplicate as described in "Cell viability staining" section for fluorescein isothiocyanate (FITC) labelled KI-67 and propidium iodide (PI) double staining. The cells cultured on six independent 2D plates were prepared as the controls (1 unstained control + 1 FITC-KI-67 stained control + 1 PI stained control + 3 FITC-KI-67 and PI double stained controls). After overnight, the cells were harvested by washing and spinning twice in 4 mL washing buffer (1× DPBS contained 1% FCS) at 384 rcf for 5 min. The supernatant was discarded and 2 mL of -20 °C 70% (v/v) ethanol was added in a dropwise manner while vortexing. The fixed cells were centrifuged at 850 rcf for 10 min after incubated at -20 °C for 2 h. Then the ethanol was removed and the cells were washed in 2 mL washing buffer twice at 850 rcf for 10 min. Cells were then suspended in 100 μL washing buffer. The cell suspensions for FITC-KI-67 staining were incubated with 5 μL FITC-labelled KI-67 monoclonal antibody (eBioScience^{TM}, Invitrogen) at room temperature in the dark for 30 min, while the others were only incubated with 5 μL washing buffer. All cells were then washed in 2mL washing buffer twice by centrifuging at 850 rcf for 10 min each. The cells for PI staining were resuspended and incubated in 250 μL PI working solution (1× DPBS contained 100 μg/mL RNase A (Qiagen), 50 μg/mL PI solution (Sigma-Aldrich), and 2 mM $MgCl_2$) at room temperature in the dark for 20 min, while the others were simply incubated in 250 μL washing buffer. After staining, the cell cycle was measured by a flow cytometer (BD, FACSCanto II Analyser).

Cell size distribution assay

Cell-gel hybrids (UE7T-13 and three different NOD MSCs (ND0302 NODs, ND0127 NODs and ND0057 NODs)) were prepared in microgel-coated 48-well plates as described in "Cell viability staining" section and incubated in a humidified atmosphere containing 5% CO_2 at 37 °C. The culture medium was changed every other day for up to 9 days. Cell-gel

hybrids were cooled at room temperature and imaged with an optical microscope on day 9. Typically, 5 images were randomly taken with a CKX41 optical microscope (Olympus) for each well and processed with image J (National Institutes of Health, USA). Subsequently, only cell area larger than 354 μm^2 was measured and number of cells with different area was presented.

The effect of microgels on cell differentiation of UE7T-13 and NOD MSCs with induction media

3D cell-gel hybrids of UE7T-13 and three different NOD MSCs (ND0303 NODs, ND0055 NODs and ND0059 NODs) in the coated 48-well plates were prepared as described in the "Cell viability staining" section. The 48-well plates were incubated in a humidified incubator containing 5% CO_2 at 37°C and the media were regularly changed every other day for up to 9 days. Cell differentiation was induced by replacing the complete medium with chondrogenic inductive media to stimulate (1) chondrogenesis (high glucose Dulbecco's Modified Eagle's Medium (DMEM-high, Sigma-Aldrich) supplemented with 1× ITS+Premix (BD Biosciences), 50 U/mL- 50 μg/mL penicillin-streptomycin (CSL), 2 mM L-glutamine, 100 μM L-ascorbate-2-phosphate (WAKO), 0.1 μM DBL™ Dexamethasone sodium phosphate (Hospira Australia), 0.125% bovine serum albumin (BSA, Sigma-Aldrich), 10 ng/mL human transforming growth factor-beta 3 (TGF-β3, Chemicon International); (2) osteogenic inductive media to stimulate osteogenesis (MEM supplemented with 5% FCS (Sigma-Aldrich), 1× ADDs, 100 μM L-ascorbate-2-phosphate, 0.1 μM Dexamethasone, 2.64 mM potassium dihydrogenphosphate (KH_2PO_4, BDH)); (3) adipogenic inductive media to stimulate adipogenesis (MEM supplemented with 10% FCS (Sigma-Aldrich), 1× ADDs, 100 μM L-ascorbate-2-phosphate, 0.1 μM Dexamethasone, 60 μM indomethacin (Sigma-Aldrich)). Cells were continuously cultured in the humidified incubator containing 5% CO_2 at 37°C for another 4 weeks with chondrogenic medium change three times weekly, while

osteogenic and adipogenic medium change twice weekly. Pellets of cells, centrifuged at 600 rcf for 5 min and cultured in a 10 mL polypropylene tube, were used as the control for 3D chondrogenesis, while cells on the 2D 96-well plate were considered as the control of 3D for osteogenesis and adipogenesis. The controls were cultured and differentiated in the same way as 3D while the microgel was replaced with Milli-Q® water. The mRNA of cells was extracted and analyzed after 37 days.

The effect of microgels on cell differentiation of UE7T-13 without induction media

3D cell-gel hybrids of UE7T-13 were prepared in microgel-coated 48-well plates as described in "Cell viability staining" section, while cell-gel hybrids were kept in the complete growth medium for up to 37 days. Cells centrifuged at 600 rcf for 5 min and cultured in a polypropylene tube were used as chondrogenic control while cells cultured on a 2D 48-well plate were used as osteogenic and adipogenic controls. The controls were cultured in the same way as cells within 3D microgel-formed constructs. After 9 days or 37 days, the mRNA of cells was extracted and analyzed.

RNA extraction

At pre-determined time points, cell-gel hybrids were harvested and centrifuged as described in the "Trypan blue cell counting and AnnexinV/7-AAD apoptosis flow cytometry" section. The cells were subsequently lysed by homogeneously mixing with 1 mL of ambion® TRIzol (Life Technologies) for 5 min at room temperature. The separated top layer was retained after addition of 200 μL chloroform and spinning at 12000 rcf for 15 min at 4 °C. Then mRNA was precipitated by addition of 1.5 μL glycogen (Roche Diagnostics) and incubating on ice for 1 hr after gently mixing with 500 μL of isopropanol. The precipitated mRNA was centrifuged at 12000 rcf for 10 min at 4 °C and washed with 75% of cold ethanol at 7500 rcf for 5 min. mRNA was dissolved in 30 μL of RNase free water at 55 °C for 10 min

after removal of all ethanol. mRNA concentration was measured by a Nanodrop spectrophotometer (Thermo Fisher Scientific).

Reverse transcription polymerase chain reaction (RT-PCR)

1 μg of extracted mRNA was homogeneously mixed with 1 μL 100 ng/mL of random primers (Geneworks) and 1 μL 10 mM of dNTPs (Adelab Scientific) and nuclease free water (Invitrogen) to a final volume of 14 μL in a PCR tube. The mixture was incubated at 65 °C for 5 min and subsequently placed on ice for 1 min by a Veriti 96 well thermal cycler (Applied Biosystems). Subsequently, the solution was homogeneously mixed with 6 μL of reverse transcriptase pre-mix (1 μL 100 mM of DTT (Thermo Fisher Scientific, Invitrogen) and 1 μL 200 U/μL of SuperScript™ IV reverse transcriptase (Thermo Fisher Scientific, Invitrogen) dissolved in 4 μL of 5x superscript IV reverse transcriptase buffer (Thermo Fisher Scientific, Invitrogen)). RT-PCR was initiated by a Veriti 96 well thermal cycler with the setting of 55 °C for 60 min and 80 °C for 10 min. After RT-PCR, the cDNA was diluted with 80 μL of nuclease free water and stored at -20 °C.

Real-time polymerase chain reaction

2 μL cDNA of each sample was mixed with 7.5 μL of RT^2 SYBR® GREEN ROX™ qPCR Mastermix (QIAGEN), 0.75 μL forward/reverse primer pair (10 μM each, gene sequence of β-actin, chondrogenic, osteogenic, and adipogenic genes as detailed in Table 1), and 4.75 μL of nuclease free water and loaded into a clear thin-walled Hard-Shell® 96-well PCR plate (BIO-RAD). The gene for each sample was prepared in triplicate and run by a CFX Connect™ Real-Time PCR Detection System (BIO-RAD). Meanwhile, nuclease free water was used as a control.

Table 1 Specific primers for reverse transcription polymerase chain reaction.

Primers	Sequence (5'→3')
β-actin	Forward: GATCATTGCTCCTCCTGAGC
	Reverse: GTCATAGTCCGCCTAGAAGCAT
SOX9	Forward: AGGTGCTCAAAGGCTACGAC
	Reverse: GCTTCTCGCTCTCGTTCAGA
Aggrecan	Forward: CTGCTTCCGAGGCATTTC
	Reverse: GCTCGGTGGTGAACTCTAGC
Collagen II	Forward: ATCACAGGCTTCCATTGACC
	Reverse: CTCCACAGCATCGATGTCAC
RUNX2	Forward: GTGGACGAGGCAAGAGTTTCA
	Reverse: CATCAAGCTTCTGTCTGTGCC
Osteocalcin	Forward: ATGAGAGCCCTCACACTCCTCG
	Reverse: GTCAGCCAACTCGTCACAGTCC
Osterix	Forward: CTGCGGGACTCAACAACTCT
	Reverse: GAGCCATAGGGGTGTGTCAT
Adipsin	Forward: GACACCATCGACCACGAC
	Reverse: CCACGTCGCAGAGAGTTC
C-ebpα	Forward: GGGCAAGGCCAAGAAGTC
	Reverse: TTGTCACTGGTCAGCTCCAG
Adiponectin	Forward: GCTGGGAGCTGTTCTACTGC
	Reverse: CGATGTCTCCCTTAGGACCA

Frozen tissue section preparation

Cell-gel hybrids of UE7T-13 or ND0303 NODs were prepared as described in "Cell viability staining" section and induced cell differentiation on day 9. Cells were cultured in chondrogenic, osteogenic, and adipogenic media for another 4 weeks, while cells cultured within the microgel with complete growth medium (without the addition of inductive media) were used as controls. After 37 days, the cells were harvested by diluting the cell-gel hybrids within cool 1×DPBS and spinning at 383 rcf for 5 min. The harvested cells were resuspended in 0.5 mL of 4% cold paraformaldehyde (PFA, Sigma-Aldrich) overnight for fixation. The cells were washed three times in 1 mL of 1×DPBS by centrifuging at 383 rcf for 10 min and immersed in 0.5 mL of 30% sucrose (Chem-Supply) overnight. The cell solution within sucrose was then transferred to the surface of a GF/C glass microfiber circle paper (Whatman, diameter of 2.1 cm) with filter papers and Kimwipes® absorbing water from the bottom. The side of the glass microfiber circle paper that contained cells were covered with one droplet of OCT compound (Tissue-Tek) and left on the working bench for 10 min. A standard pre-labeled Cryomold® (Tissue-Tek, 25mm x 20mm x 5mm) was upside down and allowed its bottom to loosely contact with the side of glass microfiber paper containing OCT. The OCT compound was topped-up on the other side of the glass microfiber paper after the Cryomold® was turned over. The Cryomold® with cells was placed on the dry ice for freezing, after which the frozen Cryomold® was covered by aluminum foil in a sealed bag and stored at -80 °C.

Prior to sectioning, the frozen OCT-embedded cells were equilibrated to -20 °C for 20 min. Cells were then sectioned onto gelatin-coated slides (dipping microscope glass slides (Livingstone) 3-5 times (5 sec each) in 0.5 % (wt/v) of gelatin (Sigma-Aldrich) and 0.05 % (wt/v) chromium potassium sulfate dodecahydrate ($CrK(SO_4)_2 \bullet 12H_2O$, Sigma-Aldrich) solution and dry at room temperature for 24 hr) at 8 μm of thickness by a Cryostat Shandon

Cryotome E (Thermo Fisher Scientific). The frozen tissue sections were kept in a sealed slide box at -80 °C.

Histological staining

Oil Red O staining

Frozen tissue slides were brought to room temperature for 1 hr and rinsed by 60% of isopropanol three times. The sectioned tissues were subsequently stained with Oil Red O working solution for 15 min, which was prepared by diluting 0.5% (wt/v) of isopropanol dissolved Oil Red O (ICN Biomedicals) stock solution in Milli-Q® water with the volumetric ratio of 3:2. Three washes in 60% of isopropanol were applied to wash out the unbound dye. The sectioned tissues were lightly stained in Mayer's hematoxylin (Fronine) by dipping the sections 5 times. The cells were "blued" by washing the sections in distilled water for 1 min. The sectioned slides were mounted with Aquatex® aqueous mountant (Merck) and covered with coverslips (Corning, 24mm x 50mm). Finally, the stained tissues were imaged with a CKX41 microscope.

Alizarin Red S staining

The frozen tissue sections were brought to room temperature for 1 hr and stained with 2% of Alizarin Red S solution (Sigma-Aldrich, pH 4.3 in Milli-Q® water) for 5 min. The sectioned tissues were, in turn, dehydrated with acetone, acetone:xylene (volumetric ratio 1:1), and xylene (three times each). The sectioned slides were mounted in the CV mountant (Leica) and covered with coverslips. Finally, the stained tissues were imaged with a CKX41 microscope.

Alcian Blue staining

The frozen tissue sections were brought to room temperature for 1 hour and stained in 1% of Alcian Blue solution (Sigma-Alrich, pH 2.5 in 3% of acetic acid) for 30 min. The sectioned tissues were counterstained with 0.1% of nuclear fast red solution (Sigma-Aldrich)

for 5 min. After staining, sectioned slides were rinsed with distilled water to remove the dyes. 70% of ethanol, 100% of ethanol, and xylene were in turn used to dehydrate the tissues. After drying in air, the sectioned slides were mounted in the CV mountant and covered with coverslips. Finally, the stained tissues were imaged with a CKX41 microscope.

Immunofluorescent staining

The frozen tissue sections were brought to room temperature for 1 hr and covered with 200 μL of 5% normal serum from the same species as secondary antibody (normal goat serum (Thermo Fisher Scientific) for chondrogenic and adipogenic sections, while normal rabbit serum (Thermo Fisher Scientific) for osteogenic sections, diluting in 0.3% of Triton x-100/1×DPBS (Sigmar-Aldrich)) per section in a humidified box at room temperature for 60 min. After the blocking solution was removed, 250 μL of collagen II A1 primary antibody from rabbit (Santa Cruz) with 1:250 dilution in 0.3 % of Triton x-100/1×DPBS was added onto each chondrogenic tissue sectioned slide, 250 μL of perilipin primary antibody from rabbit (Cell signaling) with 1:250 dilution in 0.3% of Triton x-100/1×DPBS was added onto each adipogenic tissue sectioned slide, 250 μL of osteocalcin primary antibody from goat (Santa Cruz) with 1:250 dilution in 0.3% of Triton x-100/1×DPBS was added to each osteogenic tissue sectioned slides, respectively. The tissue sections were kept in a humidified box at 4 °C overnight. Then the sections were washed 3 times in 1×DPBS after flicking away the primary antibodies. 250 μL of the secondary antibodies (fluorescein (FITC) labeled goat-anti-rabbit secondary antibody (SouthernBiotech) with 1:250 dilution in 0.3% of Triton x-100/1×DPBS for chondrogenic and adipogenic tissue sections, while FITC labeled rabbit-anti-goat secondary antibody (SouthernBiotech) with 1:250 dilution in 0.3% of Triton x-100/1×DPBS for osteogenic tissue sections) were added onto each slide and incubated at room temperature for 2 hr in a humidified box in the dark. In addition, the tissue sections were counterstained in 300 nM of DAPI (Sigma-Aldrich) for 15 min and rinsed three times in

1×DPBS for 5 min at room temperature. Finally, the tissue sections were imaged with an IX53 fluorescent microscope (Olympus) immediately after being mounted in the ProLong Gold Antifade reagent (Invitrogen) and covered with coverslips. After imaging, the tissue section slides were stored flat at 4 °C in the dark.

Statistical Analysis

All experiments were performed in triplicates. Data are presented as mean ± standard error (SE). Comparison between means was processed by one-tailed student t-test. Differences were considered as significant when $p < 0.05$, or the most significant when $p < 0.001$.

Results

Thermosensitive property of p(NIPAAm-AA).

Because of shrinkage after gelation [43], other investigators have copolymerized pNIPAAm with hydrophilic monomers to reduce the effect of syneresis.[32, 44, 45] In this study, p(NIPAAm-AA) microgel was successfully synthesized as preciously described[32]. The thermosensitive behavior, i.e. sol status at room temperature, while gelation at 37 °C (Figure S1), was confirmed by mixing 50 mg/mL of microgel with 0.05 M $MgCl_2$ dissolved in 1×DPBS and medium with a volumetric ratio of 3:1:1. Successful copolymerization of acrylic acid with N-isopropylacrylamide was confirmed with the evidence of microgel size increase in water compared to that in 1× DPBS at 25 °C (Figure S2 a). More carboxyl groups ionized in water than in 1× DPBS, which counteracted the hydrophobic effect of the backbone and increased the microgel size. However, external temperature became the dominant factor influencing the microgel size at 37 °C. Hence, no significant difference between the microgel size in water and 1× DPBS was seen. To study the reversibility of the thermosensitive behavior, the time-dependent gelation process of p(NIPAAm-AA) microgel-formed 3D constructs was also investigated by measuring the transmittance at 37 °C and 25 °C. When the constructs were transferred from room temperature to 37 °C, the transmittance gradually decreased within 5 min, while sharply dropped down from 5 min to 10 min (Figure S2 b). After 15 min, the transmittance was kept at around 0%. The p(NIPAAm-AA) microgel-formed 3D constructs formed gel completely after incubation at 37 °C for 30 min. When the temperature was changed to 25 °C, transmittance of p(NIPAAm-AA) microgel-formed constructs sharply increased within 5 min and then kept at 100%, where the p(NIPAAm-AA) microgel-formed constructs were completely liquefied. In addition, the dynamic moduli of p(NIPAAm-AA) microgel-formed 3D constructs were measured by varying external stress at a frequency of 0.1 Hz at 37 °C (Figure S2 c). When the external

stress increased above 0.12 Pa, the viscous modulus (G") became larger than the elastic modulus (G'), which was considered as the liquefied stress that transformed the gel status of the p(NIPAAm-AA) microgel-formed 3D constructs to the sol status.

No cytotoxicity of p(NIPAAm-AA) microgels to UE7T-13.

To study the cytotoxicity of the microgel to hMSCs cultured on a flat surface, different concentrations of the microgel dissolved in 1×DPBS were added to UE7T-13 pre-seeded 96 wells. The cells showed relatively high viability at a concentration ranging from 0.05 mg/mL to 5 mg/mL, while viability was reduced to 60% when the microgel was used at a concentration of 30 mg/mL (Figure S3 a). To further study the cytotoxicity of p(NIPAAm-AA) microgels to hMSCs at the concentration of 30 mg/mL, UE7T-13 were incorporated within the microgel-formed 3D constructs and cultured with complete growth medium for 24 hr. The relative cell viability was approximately 100%, irrespective of the methods for evaluating the cell viability (trypan blue staining and flow cytometry following PE-AnnexinV/7-AAD staining) (Figure S3 b). In addition, the majority of the cells cultured within the microgel-formed 3D constructs (Figure S4) remained viable after cultured in the complete growth medium for 9 days (Figure S5 a ii).

Proliferation within 3D microgel-formed constructs compared with that on 2D surfaces.

To study the cell proliferation of hMSCs within the microgel-formed constructs, UE7T-13 and primary human mesenchymal stromal cells from three different normal donors (NOD MSCs) were cultured in the 3D microgel-formed constructs with the complete growth medium for up to 14 days. Since the reduction of WST-1 to soluble formazan is linearly proportional to cell number within a certain range, cell proliferation can be determined simply from the absorbance of the soluble formazan. UE7T-13 proliferated more slowly within 3D microgel-formed constructs than on the 2D plate (Figure 1 a). This difference was the most significant when 1×10^5 cells/mL were seeded from day 1 to day 9 while relatively

significant from day 9 to day 14 (Figure 1 a). At a higher cell seeding density, 1×10^6 cells/mL, cell proliferation within the 3D microgel-formed constructs was still significantly lower than that on 2D plate throughout the 14-day culture (Figure 1 a). The results were consistent with the cell proliferation of three different NOD MSCs, which also showed a lower cell proliferation rate within the 3D microgel-formed constructs compared to the 2D plate when a seeding density of 1×10^5 cells/mL was used (Figure 1 b). Notably, this difference for NOD MSCs proliferation between 3D microgel-formed constructs and 2D culture was significant at all time points examined (Figure 1 b). After UE7T-13 cells from 2D plates and 3D microgel-formed constructs were harvested on day 1, cell surface stemness marker STRO-1 [42] was detected by flow cytometry. It was found that over 90% of cells from 2D plates and 3D microgel-formed constructs still kept STRO-1 antigen expression. There was no significant difference between both cell culture systems (Figure S6 a). To determine the reason for the low cell proliferation, cell cycle of UE7T-13 cells cultured on 2D plates and in 3D microgel-formed constructs was measured by FITC-KI-67 antibody and propidium iodide (PI) double staining flow cytometry. The result indicated that more UE7T-13 cells cultured within 3D microgel-formed constructs remained at the G0 phase of a cell cycle than those on 2D plates (Figure S6 b), while less UE7T-13 cells cultured within 3D microgel-formed constructs stayed at the S and G2/M phase of a cell cycle (Figure S6 b).

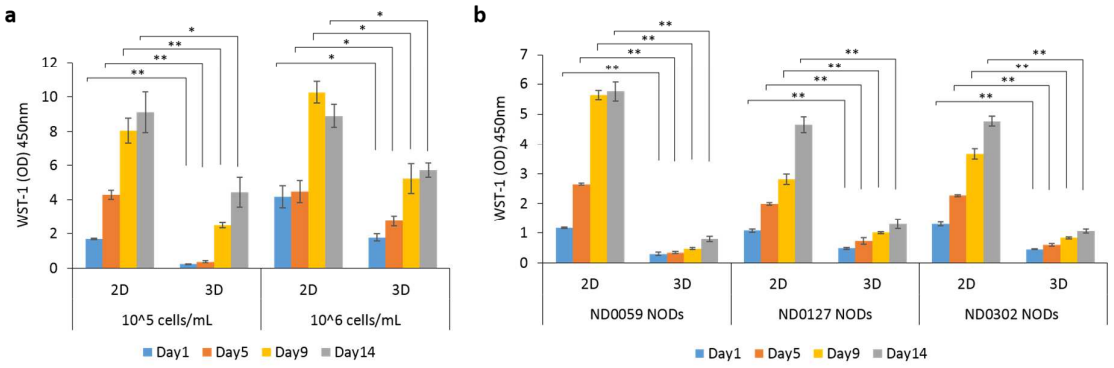

Figure 1 Proliferation of (a) UE7T-13 and (b) three NOD MSCs for 14 days. (2D: cells cultured on the multi-well plate, 3D: cells cultured within the thermosensitive p(NIPAAm-AA) microgel-formed constructs. Data were presented as the mean ± standard error (n=3). *$p < 0.05$, **$p < 0.001$.

Multi-lineage cell differentiation of UE7T-13 within 3D microgel-formed constructs in the absence of induction media.

Even though the microgel was not toxic to the hMSCs, the cell proliferation rate of UE7T-13 and NOD MSCs within 3D microgel-formed constructs was significantly lower than that observed in 2D culture (Figure 1). To determine if this reduction in cell proliferation was accompanied by an increased propensity for hMSC differentiation within 3D microgel-formed constructs, mRNA expression of UE7T-13 for a range of osteogenic, adipogenic and chondrogenic genes was measured by quantitative real time PCR after 9 days and 37 days of culture in the complete growth media. On day 9, UE7T-13 cultured in 3D microgel-formed constructs showed higher mRNA expression of chondrogenic, osteogenic and adipogenic genes than the controls (Figure 2). Particularly SOX9, aggrecan, RUNX2 and osterix exhibited significant difference between 3D and the controls. However, on day 37 only mRNA expression of aggrecan within 3D microgel-formed constructs was significantly higher than that of cell pellets cultured within polypropylene tubes (Figure 3). Notably, the mRNA expression of SOX9, collagen II, RUNX2, osteocalcin and adiponectin within 3D microgel-formed constructs on day 37 was significantly lower than that observed on day 9 (Figure 3).

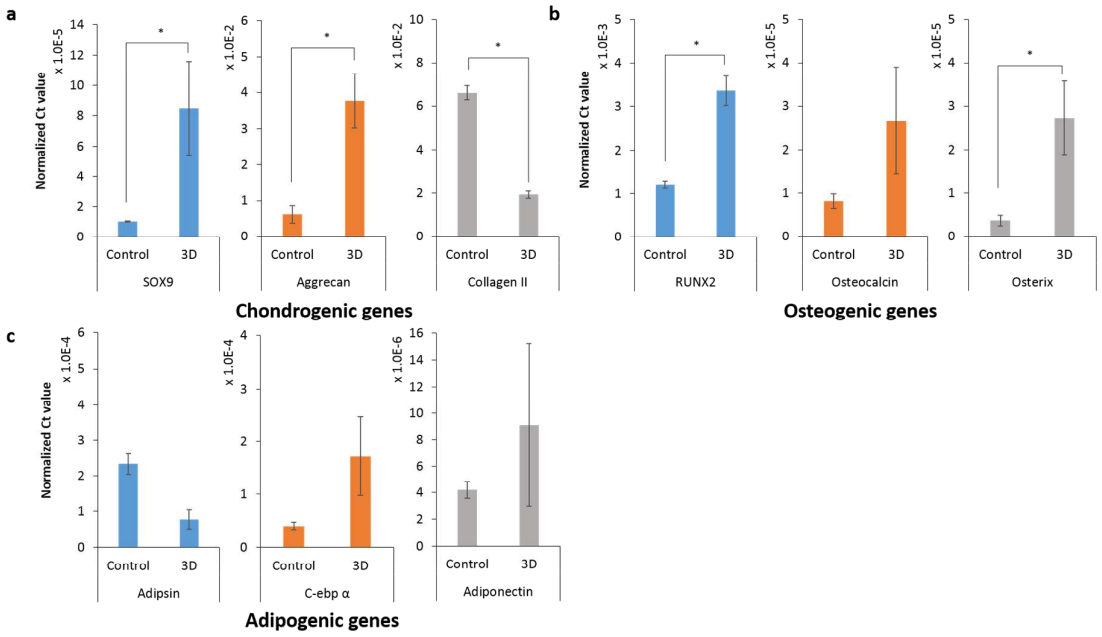

Figure 2 Cell differentiation of UE7T-13 without induction media. (a) Chondrogenic gene expression (control: cell pellets cultured in the polypropylene tube by centrifuge, 3D: cells cultured within the thermosensitive p(NIPAAm-AA) microgel-formed constructs); (b) osteogenic gene expression (control: cells cultured on the multi-well plate, 3D: cells cultured within thermosensitive p(NIPAAm-AA) microgel-formed constructs); and (c) adipogenic gene expression (control: cells cultured on the multi-well plate, 3D: cells cultured within thermosensitive p(NIPAAm-AA) microgel-formed constructs); of UE7T-13 without induction media on day 9. mRNA expression of genes were analysed by qRT-PCR and normalized to β-Actin. Data were presented as the mean ± standard error (n=3). *$p < 0.05$.

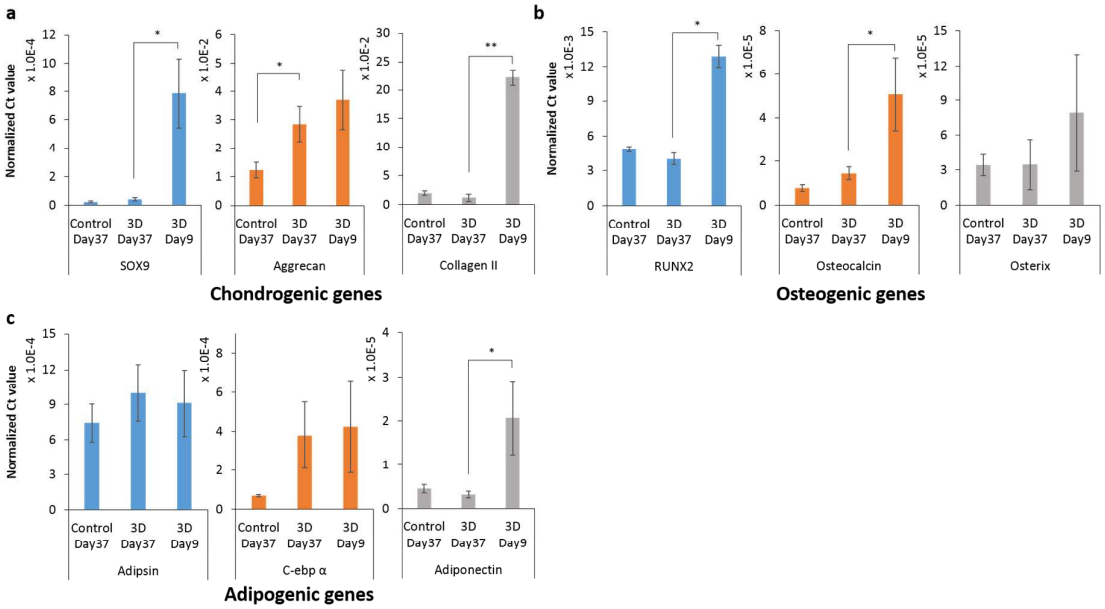

Figure 3 Cell differentiation of UE7T-13 without induction media. (a) Chondrogenic gene expression (control: cell pellets cultured in the polypropylene tube by centrifuge, 3D: cells cultured within the thermosensitive p(NIPAAm-AA) microgel-formed constructs); (b) osteogenic gene expression (control: cells cultured on the multi-well plate, 3D: cells cultured within thermosensitive p(NIPAAm-AA) microgel-formed constructs); and (c) adipogenic gene expression (control: cells cultured on the multi-well plate, 3D: cells cultured within thermosensitive p(NIPAAm-AA) microgel-formed constructs); of UE7T-13 without induction media on day 9 and day 37. mRNA expression of genes were analysed by qRT-PCR and normalized to β-Actin. Data were presented as the mean ± standard error (n=3). *$p < 0.05$, **$p < 0.001$.

Multi-lineage differentiation of hMSCs in 3D microgel-formed constructs in specific induction medium.

From the studies described in Figure 1, it was evident that the maximal proliferative activity reached on day 9 of culture, after which cell proliferation decreased. Notably, on day 9, UE7T-13 appeared to form uniform cell spheroids within the 3D microgel-formed

constructs with the help of microgel pre-coating on the culture plate on day 9 (Figure 4 a i, Figure 4 b and Figure S5 a, b).

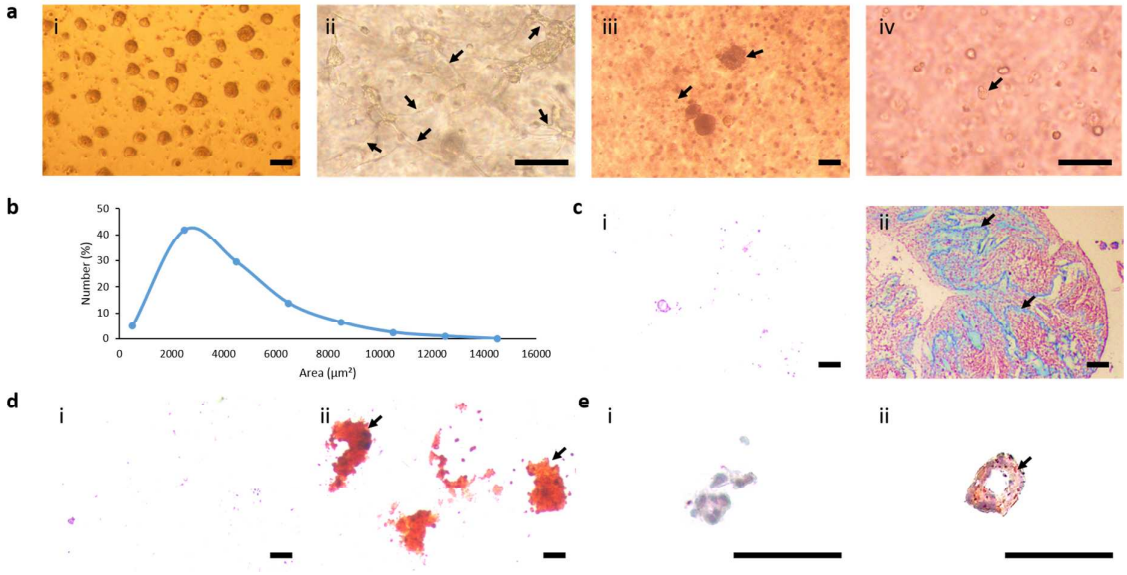

Figure 4 Differentiation of UE7T-13 cell spheroids within the thermosensitive p(NIPAAm-AA) microgel-formed constructs. (a) Optical images showed (i) generation of cell spheroids on day 9 without induction. (ii) Early connection of cell spheroids on day 37 within chondrogenic medium (Arrows point to the inter-spheroid connection sites). (iii) Mineralization of cell spheroids on day 37 within osteogenic medium (Arrows point to the mineralized cell spheroids). (iv) Lipids formation on day 37 within adipogenic medium (Arrow points to the lipids). (b) Size distribution of cell spheroids on day 9 without induction (n=3, where five optical imaged were randomly taken for each and measured by image J). (c) Histological images of (i) no-induction and (ii) induction in chondrogenic medium by Alcian blue staining on day 37 (Red-nuclei; Blue-glycosaminoglycans (GAGs); Arrows point to the GAGs sites). (d) Histological images of (i) no-induction and (ii) induction in osteogenic medium by Alizarin red S staining on day 37 (Red-calcium deposition; Arrows point to the deposited calcium sites). (e) Histological images of (i) no-induction and (ii) induction in

adipogenic medium by Oil red O staining on day 37 (Blue-nuclei; Red-lipids; Arrow points to the lipid within the cells). Scale bar: 100 μm.

UE7T-13 cells were cultured for 9 days and the cell differentiation was induced within chondrogenic, osteogenic or adipogenic induction media. After further 4 weeks of culture, the cells were harvested and lysed for the study of mRNA expression. Chondrogenic genes (SOX9, aggrecan and collagen II) and osteogenic genes (RUNX2 and osteocalcin) and adipogenic genes (adipsin, c-ebp α and adiponectin) within 3D microgel-formed constructs all showed significantly higher mRNA expression than the controls (Figure 5), confirming that the 3D microgel promoted hMSC differentiation.

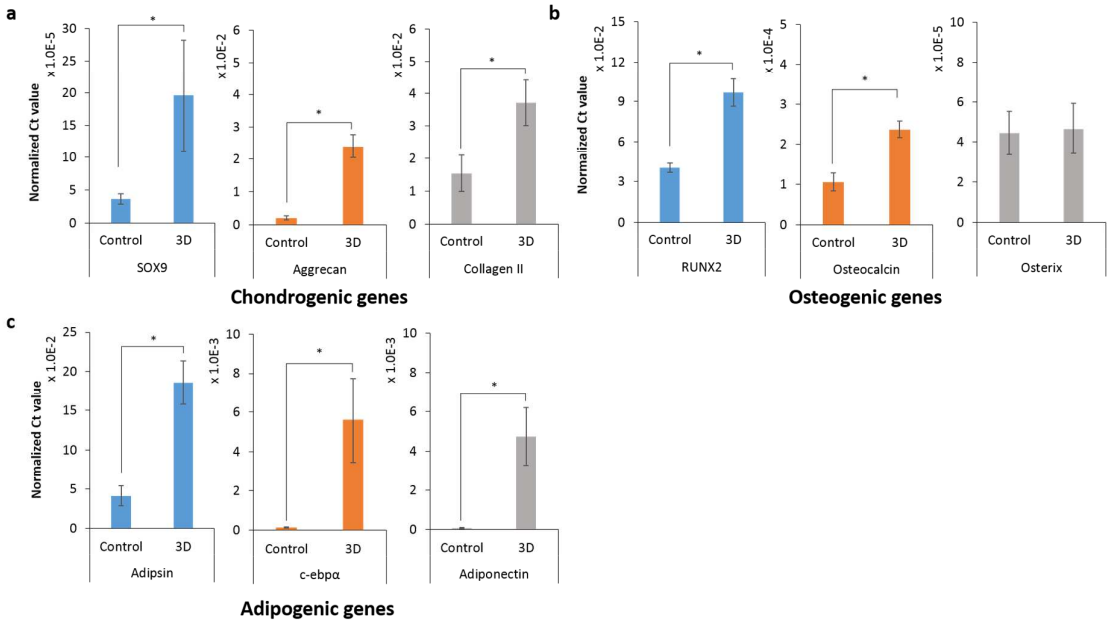

Figure 5 Cell differentiation of UE7T-13 with induction media. (a) Chondrogenic gene expression (control: cell pellets cultured in the polypropylene tube by centrifuge, 3D: cells cultured within the thermosensitive p(NIPAAm-AA) microgel-formed constructs); (b) osteogenic gene expression (control: cells cultured on the multi-well plate, 3D: cells cultured within thermosensitive p(NIPAAm-AA) microgel-formed constructs); and (c) adipogenic gene expression (control: cells cultured on the multi-well plate, 3D: cells cultured within

thermosensitive p(NIPAAm-AA) microgel-formed constructs); of UE7T-13 with induction media on day 37 by adding specific induction media on day 9. mRNA expression of genes were analysed by qRT-PCR and normalized to β-Actin. Data were presented as the mean ± standard error (n=3). *$p < 0.05$.

Human patient-derived hMSC from three different normal donors (NOD MSCs) were cultured within the 3D microgel-formed constructs. Cell spheroids of NOD MSCs were successfully formed after one day of culture (Figure 6 a i), which continued to increase after 9-day culture with the complete growth medium (data not shown). The size of NOD MSC spheroids from three different normal donors on day 1 were uniformly distributed and were similar to that of UE7T-13 on day 9 (Figure 6 b).

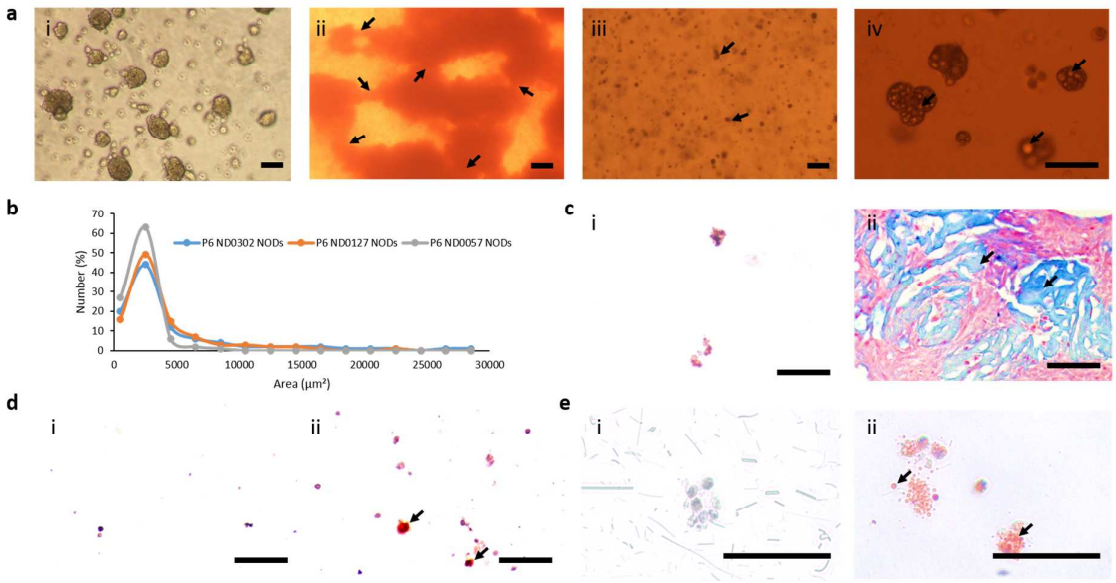

Figure 6 Differentiation of NOD MSC spheroids within the thermosensitive p(NIPAAm-AA) microgel-formed constructs. (a) Optical images showed (i) generation of cell spheroids on day 1 without induction. (ii) Inter-spheroid connection of cell spheroids on day 37 within chondrogenic medium (Arrows point to the connection sites). (iii) Mineralization of cell spheroids on day 37 within osteogenic medium (Arrows point to the mineralized cell spheroids) (iv) Lipids formation on day 37 within adipogenic medium (Arrows point to the

lipids). (b) Size distribution of cell spheroids on day 1 without induction (n=3, where five optical imaged were randomly taken for each and measured by image J). (c) Histological images of (i) no-induction and (ii) induction in chondrogenic medium by Alcian blue staining on day 37 (Red-nuclei; Blue-glycosaminoglycans (GAGs); Arrows point to the GAGs sites). (d) Histological images of (i) no-induction and (ii) induction in osteogenic medium by Alizarin red S staining on day 37 (Red-calcium deposition; Arrows point to the deposited calcium sites). (e) Histological images of (i) no-induction and (ii) induction in adipogenic medium by Oil red O staining on day 37 (Blue-nuclei; Red-lipids; Arrows point to the lipid within the cells). Scale bar: 100 μm.

NOD MSCs were subsequently cultured in the induction media on day 9 for up to 37 days. After induction for 4 weeks, quantitative PCR was performed to measure the mRNA expression of specific genes within NOD MSCs. mRNA expression of SOX9, aggrecan, RUNX2, osterix and c-ebp α from three different normal donors was significantly higher within 3D microgel-formed constructs than the 2D controls. Similar differences were observed for mRNA expression of adipsin and adiponectin within 3D microgel-formed constructs (Figure 7). However, due to normal donor cell variation, only NOD MSCs from two different normal donors (ND0303 NODs and ND0059 NODs) displayed significant difference between 3D and the 2D controls (Figure 7).

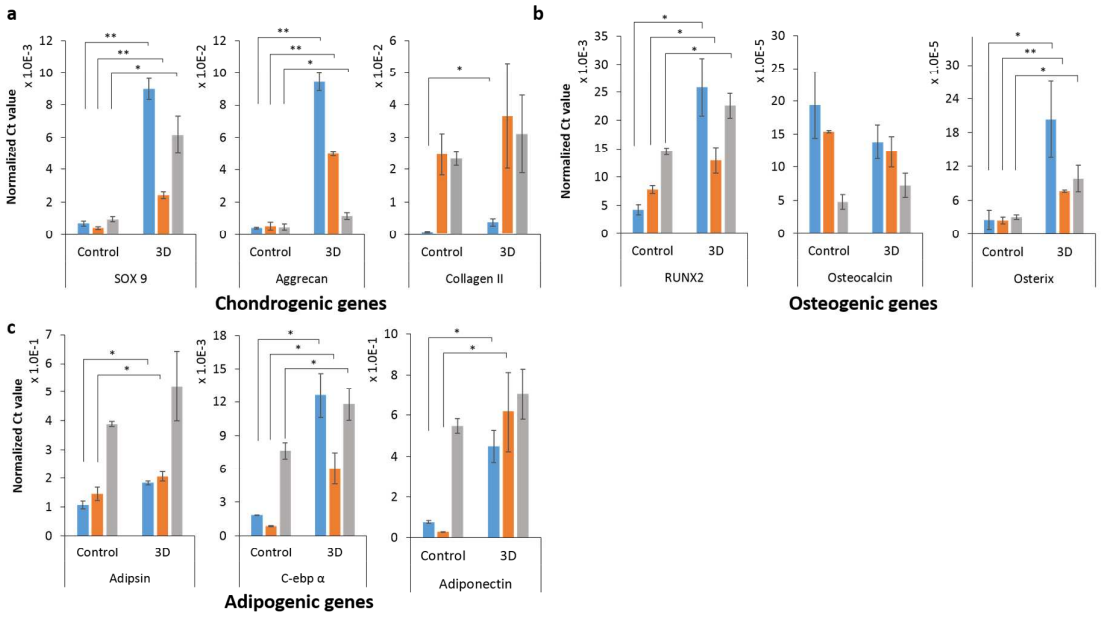

Figure 7 (a) Chondrogenic gene (control: cell pellets cultured in the polypropylene tube by centrifuge, 3D: cells cultured within the thermosensitive p(NIPAAm-AA) microgel-formed constructs); (b) osteogenic gene (control: cells cultured on the multi-well plate, 3D: cells cultured within thermosensitive p(NIPAAm-AA) microgel-formed constructs); and (c) adipogenic gene expression (control: cells cultured on the multi-well plate, 3D: cells cultured within thermosensitive p(NIPAAm-AA) microgel-formed constructs) of three NOD MSCs on day 37 by adding specific induction media on day 9. Blue: ND0303 NODs; orange: ND0059 NODs; grey: ND0055 NODs. mRNA expression of genes was analysed by qRT-PCR and normalized to β-Actin. Data were presented as the mean ± standard error (n=3). *$p < 0.05$, ** $p < 0.001$.

Evident staining of differentiated hMSCs within 3D microgel-formed constructs.

To further confirm the multi-lineage differentiation of human stem cells within 3D microgel-formed constructs, both histological and immunofluorescent staining were performed for UE7T-13 and NOD MSCs. Mineralization within osteogenic groups (Figure 4 a iii and Figure 6 a iii), and lipids within adipogenic groups (Figure 4 a iv and Figure 6 a iv)

were evident by a optical microscope prior to any staining. Chondrogenic differentiation, as marked Alcian Blue staining of glycosaminoglycan (GAG) expression, a significant component of cartilage, was evident in hMSCs cultured in the 3D microgel-formed constructs (Figure 4 c and Figure 6 c). UE7T-13 and NOD MSCs, cultured within the 3D microgel-formed constructs for 37 days without induction medium, formed small cell spheroids and showed no visible blue staining (Figure 4 c i and Figure 6 c i), while cells cultured within the 3D microgel-formed constructs in chondrogenically inductive media for 4 weeks formed a more complex micro-tissue and showed rich blue-staining GAGs among the micro-tissue section (Figure 4 c ii and Figure 6 c ii). Moreover, UE7T-13 and NOD MSCs cultured within 3D microgel-formed constructs in osteogenic-induction media for 4 weeks showed distinct red by Alizarin Red S staining as evidence of calcification (Figure 4 d ii and Figure 6 d ii). On contrary, cells cultured within 3D microgel-formed constructs with the complete growth medium for up to 37 days were not stained red by Alizarin Red S (Figure 4 d i and Figure 6 d i). Furthermore, lipids were only found for cells cultured with adipogenic-induction medium for up to 37 days (Figure 4 e and Figure 6 e) by Oil Red O staining.

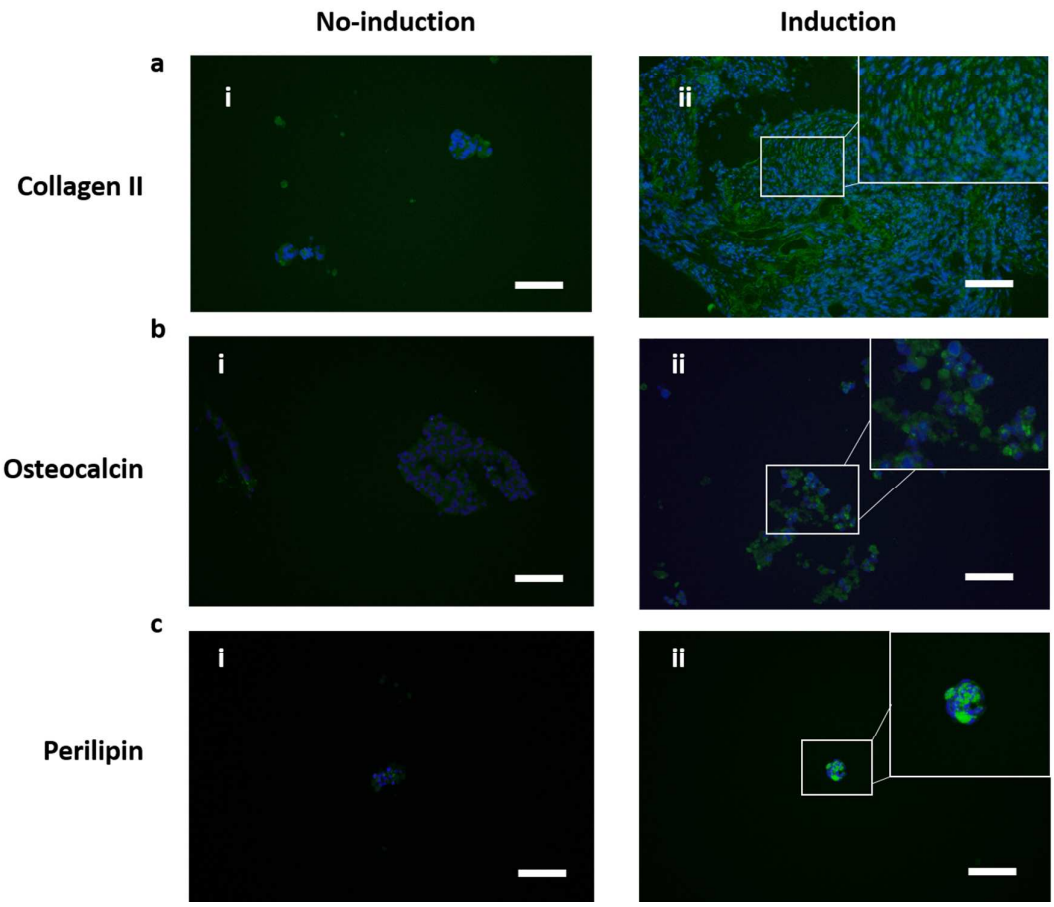

Figure 8 Immunofluorescent images of UE7T-13 within the thermosensitive p(NIPAAm-AA) microgel-formed constructs on day 37. (a) Collagen II A1 expression of (i) no-induction and (ii) induction in chondrogenic medium (Blue-DAPI; Green-collagen II A1). (b) Osteocalcin expression of (i) no-induction and (ii) induction in osteogenic medium (Blue-DAPI; Green-osteocalcin). (c) Perilipin expression of (i) no-induction and (ii) induction in adipogenic medium (Blue-DAPI; Green-perilipin). Scale bar: 100 μm.

Immunofluorescent staining of collagen II A1, osteocalcin, and perilipin was also performed to confirm the multi-lineage differentiation of hMSCs in 3D microgel-formed constructs. The green FITC-labeled collagen II A1 was well distributed within the chondrogenesis-induced microtissue and much more distinct than cells within 3D microgel-formed constructs without induction (Figure 8 a and Figure 9 a). In addition, distinguishable

osteocalcin (Figure 8 b and Figure 9 b) and perilipin (Figure 8 c and Figure 9 c) expression was observed for UE7T-13 and NOD MSCs with induction media on day 37 as evidenced by the green staining, indicative of osteogenic and adipogenic differentiation, respectively. However, neither FITC-osteocalcin signal nor FITC-perilipin signal was detected for UE7T-13 and NOD MSCs cultured in the p(NIPAAm-AA) microgel-formed 3D constructs with only complete growth medium on day 37.

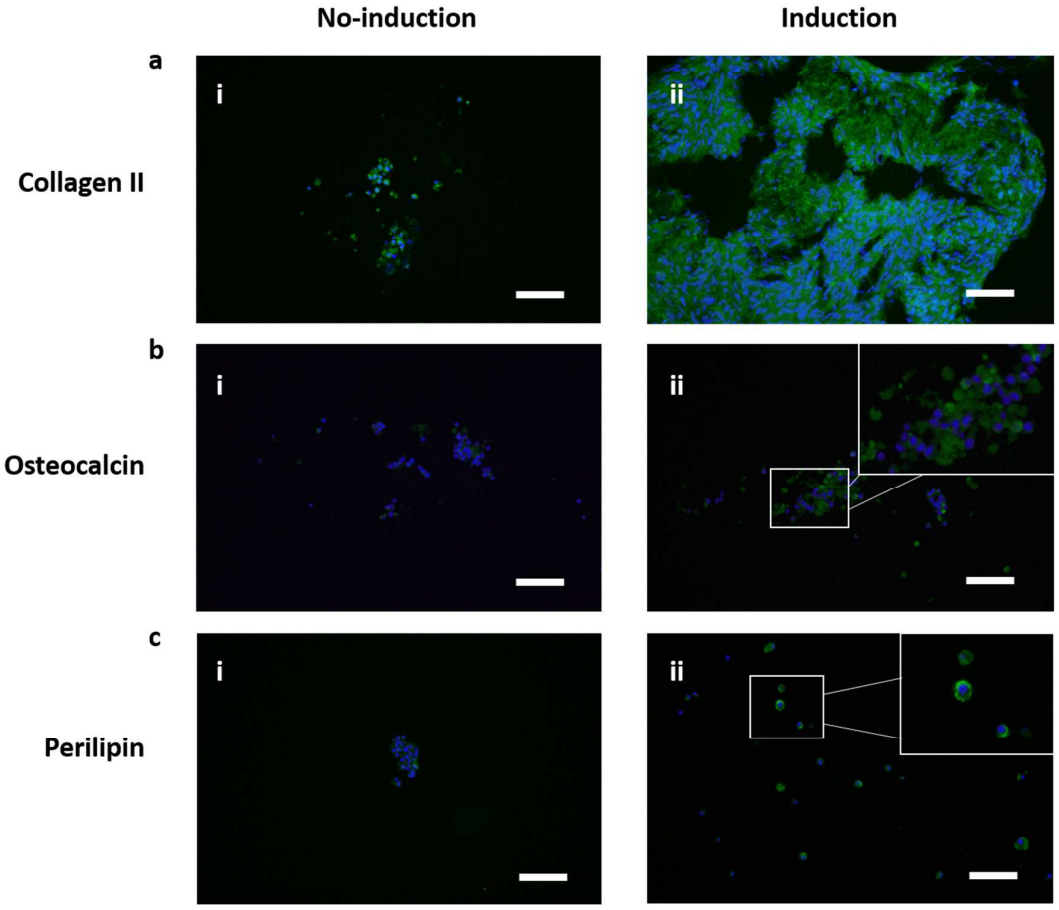

Figure 9 Immunofluorescent images of NOD MSCs within the thermosensitive p(NIPAAm-AA) microgel-formed constructs on day 37. (a) Collagen II A1 expression of (i) no-induction and (ii) induction in chondrogenic medium (Blue-DAPI; Green-collagen II A1). (b) Osteocalcin expression of (i) no-induction and (ii) induction in osteogenic medium

(Blue-DAPI; Green-osteocalcin). (c) Perilipin expression of (i) no-induction and (ii) induction in adipogenic medium (Blue-DAPI; Green-perilipin). Scale bar: 100 μm.

Discussion

The thermosensitive property of the p(NIPAAm-AA) microgel was mainly maintained by the hydrophobic interaction and physical ionic crosslinking. [44] Hence, the reversibility of sol and gel transformation, on the one hand, could be controlled by the external temperature change, which influenced the hydrophobicity of p(NIPAAm-AA). When the temperature was increased to 37 °C, the hydrophobic interaction between the p(NIPAAm-AA) was enhanced leading to the shrinkage of microgels. Then water was expelled from the center of the microgels, which made the constructs cloudy, while the forming Mg^{2+}/COO^{-} physical ionic bonding promoted the gel formation and further decreased the transmittance of the constructs (Figure S2 b). The liquefied process of p(NIPAAm-AA) microgel-formed 3D constructs was contrary to the gelation process. On the other hand, the external stress can also induce the p(NIPAAm-AA) transform from gel status, where elastic modulus (G') was higher than the viscous modulus (G") (G'>G"), to sol status, where elastic modulus was lower than viscous modulus (G'<G"), by breaking down the physical ionic crosslinking (Figure S2 c). When the external force was absent, physical ionic crosslinking could be easily formed, making the p(NIPAAm-AA) gelate again at 37 °C.

While p(NIPAAm-AA) thermosensitive 3D microgels have been previously demonstrated to support 3D culture of murine embryonic mesenchymal progenitor cells (C3H/10T1/2) and the cell proliferation within 3D microgel-formed constructs was higher than 2D plate [32], human MSCs have not been previously examined. Hence, in this study, UE7T-13 and NOD MSCs were used to assess the biological performance of p(NIPAAm-AA) microgels. From the surface toxicity assay, no toxicity of the microgel for the UE7T-13 was observed at concentrations ranging from 0.05 mg/mL to 5 mg/mL (Figure S3 a), with greater than 90% of cells remaining viable after 24 hr of culture. However, the cell viability decreased to approximately 60% with an increase in microgel concentration to 30 mg/mL. To eliminate

influence of pH change caused by the ionization of carboxyl group within p(NIPAAm-AA), p(NIPAAm-AA) microgel was dissolved in 1×DPBS and cultured overnight in complete growth medium prior to the addition of cells. We found that the microgel could not gel at 37 °C in the complete growth media. Instead, the viscous microgel was found to cover the adherent UE7T-13 and hinder the gas and mass exchange between the cells and the surrounding medium resulting in a reduced cell viability at the microgel concentration of 30 mg/mL. This assertion was supported by our previous studies which showed that p(NIPAAm) hydrogel at concentrations below 30 mg/mL did not increase apoptosis or necrosis (Figure S3 b). [46]

When UE7T-13 and NOD MSCs were incorporated within the 3D microgel-formed constructs and cultured with the complete growth medium for up to 14 days, the cells displayed reduced cell proliferation compared with cells cultured in 2D. This was most evident when NOD MSCs, were cultured in 3D microgel-formed constructs (Figure 1). These findings were contrary to our previously published findings [32]. This difference might be related to the fact that cell adhesion and active migration could be limited in soft 3D hydrogels [47, 48], particularly for p(NIPAAm)-based microgels with lack of binding sites [49]. Moreover, previous studies also suggested that human MSCs typically generated less ECM [50], suggesting that cell proliferation and survival were only possible when hMSCs formed cell spheroids within the soft 3D microgel-formed constructs [16, 51]. However, passive mass and gas diffusion within cell spheroids might be limited as the cell condensation and an increase in the cell spheroids size. [52] Furthermore, since the stiffness of p(NIPAAm-AA) microgel-formed constructs was low [32] and the microgel-cell hybrids were free-floating in culture medium, human MSCs became quiescent under such an environment [53] (Figure S6 b). Consequently, their proliferation was suppressed in the 3D microgel-formed constructs at a rate of around half of that observed in 2D cultures on day 1 (Figure 1). Once cell spheroids

were formed, stem cell differentiation was enhanced by the elevated secretion of endogenous growth factors and ECM proteins. [16] Uniform UE7T-13 spheroids within 3D microgel-formed constructs showed significantly higher mRNA expression of chondrogenic genes (SOX9 and aggrecan) and osteogenic genes (RUNX2 and osterix) on day 9 (Figure 2) compared to the controls even without induction media, while the difference was only seen for the mRNA expression of aggrecan on day 37 (Figure 3 a). It was reported that size of cell spheroids would decrease after reaching the maximal size [16, 49, 54], which were also confirmed in cell spheroids cultured on low attachment plates (Figure S5 c) and in the 15 mL polypropylene tubes (Figure S5 d) in this study. When most of UE7T-13 spheroids decreased and broke down into individual cells on day 37 (Figure 4 c i and Figure 6 c i), the functional enhancement of cell spheroids was lost, leading to a reduction of mRNA expression of chondrogenic genes (SOX9 and collagen II), osteogenic genes (RUNX2 and osteocalcin) and adipogenic genes (adiponectin) compared to those observed on day 9 (Figure 3). However, since the progress of cell spheroids formation within 3D microgel-formed constructs was slower than that on a low attachment plate and from the force-spinning (Figure S5), cell spheroids continued to increase in size even after cell induction, which maintained functional enhancement of cell spheroids to continuously up-regulate the mRNA expression of chondrogenic, osteogenic and adipogenic genes (Figure 5 and Figure 7). The benefit of cell spheroids was more distinct for the mRNA expression of collagen II, which showed a significantly higher value for the 3D than the control on day 37 (Figure 5 a), while the difference was reverse on day 9 (Figure 2 a). In addition, the progression of increasing cell spheroid in size also allows more efficient supply of inductive and/or biochemical stimuli to stem cells due to the higher surface area of small cell spheroids than that of large cell pellets. Hence, hMSCs cells within 3D microgel-formed constructs showed a significant increase in chondrogenesis, osteogenesis and adipogenesis compared to the controls.

In addition, cell spheroids within 3D microgel-formed constructs even established inter-spheroid connections to form a network during chondrogenesis (Figure 4 a ii and Figure 6 a ii). This inter-spheroid connectivity was more evident for NOD MSCs compared with UE7T-13, with evidence of a stronger network seen in chondrogenic NOD MSCs (Figure 6 a ii). This may be related to the fact that the NOD MSCs were freshly isolated from human bones and would be easily adapted to the 3D environment *in vitro*, while UE7T-13 were already modified and adapted to the 2D plate after many passages. [55] We noted that the cell spheroid network started to contract and formed a porous chondrogenic micro-tissue (Figure 4 c ii and Figure 6 c ii). Since the major components of ECM within cartilage are acidic polysaccharides [56], such as glycosaminoglycans (GAGs) and collagen II, Alcian Blue was used to distinguish and stain GAGs. It was shown that GAGs with distinct blue color were well distributed in the chondrogenic micro-tissue of UE7T-13 and NOD MSCs (Figure 4 c and Figure 6 c). In addition, abundant collagen II A1 was also labeled with green FITC-secondary antibody within the chondrogenic micro-tissue of UE7T-13 and NOD MSCs (Figure 8 a ii and Figure 9 a ii). The chondrogenic micro-tissue formed within the 3D microgel-formed constructs was similar to that formed by pellet culture [57], while the chondrogenic progress of hMSCs in the 3D microgel-formed constructs was more consistent with that *in vivo* [58]. Moreover, calcification (Figure 4 a iii and Figure 6 a iii) and lipids (Figure 4 a iv and Figure 6 a iv) were seen in the optical images of osteogenic and adipogenic cells and evidenced by Alizarin Red S staining (Figure 4 d ii and Figure 6 d ii) and Oil Red O staining (Figure 4 e ii and Figure 6 e ii), respectively. Furthermore, osteocalcin, an osteogenesis-relative protein, and perilipin, a lipid droplet-associated protein, were both clearly labeled by FITC-secondary antibody and distinguished as green in immunofluorescent images within UE7T-13 (Figure 8 b ii and Figure 8 c ii) and NOD MSCs (Figure 9 b ii and Figure 9 c ii) after specific induction. Herein, we confirm that multi-lineage differentiation of

human mesenchymal stromal cells is successfully induced in 3D microgel-formed constructs with the specific induction media. Moreover, UE7T-13 cultured in the p(NIPAAm-AA) microgel-formed constructs without induction media showed relatively high mRNA expression of aggrecan on day 9 and 37(Figure 2 a and Figure 3 a), and some chondrogenic staining (FITC-collagen II in Figure 8 a i and Figure 9 a i) on day 37, which indicated that the p(NIPAAm-AA) microgel-formed constructs could selectively promote hMSCs chondrogenesis. It was believed that the distinct chondrogenic induction was due to the synergy of cell spheroids, induction medium and environment formed by the p(NIPAAm-AA) microgels. These experimental results support that human mesenchymal stem/stromal cells within the 3D microgel-formed constructs can be efficiently induced for multi-lineage differentiation. Hence, the p(NIPAAm-AA) microgel can be potentially used as an *in-vitro* model for cell differentiation and tissue engineering or transplanted *in-vivo* into patients for specific lineage differentiation.

Conclusions

In this study, we demonstrated that the p(NIPAAm-AA) thermosensitive microgel was not toxic to human mesenchymal stromal cells and facilitated formation of uniform cell spheroids within the 3D microgel-formed constructs. The spheroid formation within the 3D microgel-formed constructs significantly up-regulated mRNA expression of chondrogenic genes (SOX9 and aggrecan) and osteogenic genes (RUNX2 and osterix) in UE7T-13 even without the induction media, but the free-floating soft microgel-formed constructs and the cell spheroids led to slow cell proliferation. When induction media were supplied *in situ*, the mRNA expression of chondrogenic, osteogenic and adipogenic genes within UE7T-13 and NOD MSCs has been significantly up-regulated. Successful cell differentiation was confirmed as evidenced by Alcian Blue stained GAGs and FITC-secondary antibody labeled collagen II A1 within the chondrogenic micro-tissue, Alizarin Red S stained calcification and FITC-secondary antibody labeled osteocalcin within osteogenic cells, and Oil Red O stained lipids and FITC-secondary antibody labeled perilipin. Hence, we concluded that highly efficient multi-lineage differentiation of human mesenchymal stromal cells can be achieved within the 3D thermosensitive microgel-formed constructs.

SUPPLEMENTARY INFORMATION

For further details of (1) thermosensitive behavior of p(NIPAAm-AA) microgel-formed constructs (Figure S1); (2) Size distribution of the microgel, time-dependent gelation process, and the stress-dependence of dynamic moduli of p(NIPAAm-AA) (Figure S2); (3) UE7T-13 viability assay after 24 hr (Figure S3); (4) SEM images of cell-gel 3D constructs (Figure S4); (5) Live&Dead staining of UE7T-13 in different culture systems (Figure S5); and (6) Cell stemness and cell cycle assay (Figure S6), please refer to the "Supplementary Information".

CONFLICTS OF INTEREST

There are no conflicts to declare.

ACKNOWLEDGEMENTS

HZ would like to acknowledge the financial support from ARC Discovery Project (DP160104632) and The Medical Advancement Without Animal (MAWA) Trust. JBZ thanks the IPE-UoA Scholarship (BES).

REFERENCES

1. A. Arthur, A. Zannettino and S. Gronthos, *Journal of Cellular Physiology*, 2009, 218, 237-245.

2. J. E. Frith, A. R. Cameron, D. J. Menzies, P. Ghosh, D. L. Whitehead, S. Gronthos, A. C. W. Zannettino and J. J. Cooper-White, *Biomaterials*, 2013, 34, 9430-9440.

3. R. C. McCarty, C. J. Xian, S. Gronthos, A. C. W. Zannettino and B. K. Foster, *The Open Orthopaedics Journal*, 2010, 4, 204-210.

4. J. E. Frith, D. J. Menzies, A. R. Cameron, P. Ghosh, D. L. Whitehead, S. Gronthos, A. C. W. Zannettino and J. J. Cooper-White, *Biomaterials*, 2014, 35, 1150-1162.

5. G. Tony, O. David, G. Peter, Z. Andrew, R. Jeffrey Victor and J. Graham, *Current Stem Cell Research & Therapy*, 2013, 8, 381-393.

6. B. J. C. Freeman, J. S. Kuliwaba, C. F. Jones, C. C. Shu, C. J. Colloca, M. R. Zarrinkalam, A. Mulaibrahimovic, S. Gronthos, A. C. W. Zannettino and S. Howell, *Spine*, 2016, 41, 1331-1339.

7. J. D. Richardson, A. J. Nelson, A. C. W. Zannettino, S. Gronthos, S. G. Worthley and P. J. Psaltis, *Stem Cell Reviews and Reports*, 2013, 9, 281-302.

8. P. J. Psaltis, A. C. W. Zannettino, S. G. Worthley and S. Gronthos, *Stem cells (Dayton, Ohio)*, 2008, 26, 2201-2210.

9. P. J. Psaltis, A. Carbone, A. J. Nelson, D. H. Lau, T. Jantzen, J. Manavis, K. Williams, S. Itescu, P. Sanders, S. Gronthos, A. C. W. Zannettino and S. G. Worthley, *JACC: Cardiovascular Interventions*, 2010, 3, 974-983.

10. K.-H. Wu, C. Mei, C.-W. Lin, K.-C. Yang and J. Yu, *Journal of Materials Chemistry B*, 2018, DOI: 10.1039/C7TB02244A.

11. E. A. Aisenbrey and S. J. Bryant, *Journal of materials chemistry. B, Materials for biology and medicine*, 2016, 4, 3562-3574.

12. A. Paul, V. Manoharan, D. Krafft, A. Assmann, J. A. Uquillas, S. R. Shin, A. Hasan, M. A. Hussain, A. Memic, A. K. Gaharwar and A. Khademhosseini, *Journal of materials chemistry. B, Materials for biology and medicine*, 2016, 4, 3544-3554.

13. Y. Hu, W. Gao, F. Wu, H. Wu, B. He and J. He, *Journal of Materials Chemistry B*, 2016, 4, 3504-3508.

14. X. Xiao, L. Yu, Z. Dong, R. Mbelek, K. Xu, C. Lei, W. Zhong, F. Lu and M. Xing, *Journal of Materials Chemistry B*, 2015, 3, 5635-5644.

15. A. Goldberg, K. Mitchell, J. Soans, L. Kim and R. Zaidi, *Journal of orthopaedic surgery and research*, 2017, 12, 39.

16. S. Sart, A. C. Tsai, Y. Li and T. Ma, *Tissue Eng Part B Rev*, 2014, 20, 365-380.

17. X. Cui, Y. Hartanto and H. Zhang, *Journal of The Royal Society Interface*, 2017, 14.

18. T. J. Bartosh, J. H. Ylöstalo, A. Mohammadipoor, N. Bazhanov, K. Coble, K. Claypool, R. H. Lee, H. Choi and D. J. Prockop, *Proceedings of the National Academy of Sciences*, 2010, 107, 13724-13729.

19. O. Jeon, R. Marks, D. Wolfson and E. Alsberg, *Journal of Materials Chemistry B*, 2016, 4, 3526-3533.

20. T. Takei, J. Kitazono, S. Tanaka, H. Nishimata and M. Yoshida, *Artif Cells Nanomed Biotechnol*, 2016, 44, 62-65.

21. H. Page, P. Flood and E. G. Reynaud, *Cell Tissue Res*, 2013, 352, 123-131.

22. S. Muduli, H. H.-C. Lee, J.-S. Yang, T.-Y. Chen, A. Higuchi, S. S. Kumar, A. A. Alarfaj, M. A. Munusamy, G. Benelli, K. Murugan, C.-Y. Liu, Y.-F. Chen, Y. Chang, B. Moorthy, H.-C. Wang, S.-T. Hsu and Q.-D. Ling, *Journal of Materials Chemistry B*, 2017, 5, 5345-5354.

23. M. Akhmanova, E. Osidak, S. Domogatsky, S. Rodin and A. Domogatskaya, *Stem Cells International*, 2015, 2015, 35.

24. M. H. Hettiaratchi, R. E. Guldberg and T. C. McDevitt, *Journal of Materials Chemistry B*, 2016, 4, 3464-3481.

25. A. Higuchi, Q.-D. Ling, S. S. Kumar, Y. Chang, A. A. Alarfaj, M. A. Munusamy, K. Murugan, S.-T. Hsu and A. Umezawa, *Journal of Materials Chemistry B*, 2015, 3, 8032-8058.

26. N. Eslahi, M. Abdorahim and A. Simchi, *Biomacromolecules*, 2016, 17, 3441-3463.

27. J. Zhang, H. Zhang and X. Xu, in *Smart Materials for Tissue Engineering: Applications*, The Royal Society of Chemistry, 2017, DOI: 10.1039/9781788010542-00473, pp. 473-504.

28. R. L. Sala, M. Y. Kwon, M. Kim, S. E. Gullbrand, E. A. Henning, R. L. Mauck, E. R. Camargo and J. A. Burdick, *Tissue Engineering Part A*, 2017, 23, 935-945.

29. S. R. Caliari and J. A. Burdick, *Nature Methods*, 2016, 13, 405.

30. P.-Y. Wang, H. H.-c. Lee, A. Higuchi, Q.-D. Ling, H.-R. Lin, H.-F. Li, S. Suresh Kumar, Y. Chang, A. A. Alarfaj, M. A. Munusamy, D.-C. Chen, S.-T. Hsu, H.-C. Wang, H.-Y. Hsiao and G.-J. Wu, *Journal of Materials Chemistry B*, 2015, 3, 3858-3869.

31. V. Rai, M. F. Dilisio, N. E. Dietz and D. K. Agrawal, *J Biomed Mater Res A*, 2017, 105, 2343-2354.

32. Z. Shen, J. Bi, B. Shi, D. Nguyen, C. J. Xian, H. Zhang and S. Dai, *Soft Matter*, 2012, 8, 7250-7257.

33. E. Smith, J. Yang, L. McGann, W. Sebald and H. Uludag, *Biomaterials*, 2005, 26, 7329-7338.

34. Z. Ren, Y. Wang, S. Ma, S. Duan, X. Yang, P. Gao, X. Zhang and Q. Cai, *ACS Applied Materials & Interfaces*, 2015, 7, 19006-19015.

35. A. Mellati, M. V. Kiamahalleh, S. H. Madani, S. Dai, J. Bi, B. Jin and H. Zhang, *Journal of Biomedical Materials Research Part A*, 2016, 104, 2764-2774.

36. A. Mellati, C.-M. Fan, A. Tamayol, N. Annabi, S. Dai, J. Bi, B. Jin, C. Xian, A. Khademhosseini and H. Zhang, *Biotechnology and Bioengineering*, 2017, 114, 217-231.

37. Y. Xu, Z. Li, X. Li, Z. Fan, Z. Liu, X. Xie and J. Guan, *Acta Biomaterialia*, 2015, 26, 23-33.

38. A. Navaei, D. Truong, J. Heffernan, J. Cutts, D. Brafman, R. W. Sirianni, B. Vernon and M. Nikkhah, *Acta Biomaterialia*, 2016, 32, 10-23.

39. Z. Dai, Y. Shu, C. Wan and C. Wu, *Journal of biomaterials applications*, 2015, 29, 1272-1283.

40. M. Zscharnack, P. Hepp, R. Richter, T. Aigner, R. Schulz, J. Somerson, C. Josten, A. Bader and B. Marquass, *The American Journal of Sports Medicine*, 2010, 38, 1857-1869.

41. G. J. Atkins, P. Kostakis, B. Pan, A. Farrugia, S. Gronthos, A. Evdokiou, K. Harrison, D. M. Findlay and A. C. Zannettino, *Journal of bone and mineral research : the official journal of the American Society for Bone and Mineral Research*, 2003, 18, 1088-1098.

42. S. Fitter, S. Gronthos, S. S. Ooi and A. C. W. Zannettino, *Stem cells (Dayton, Ohio)*, 2017, 35, 940-951.

43. I. Bischofberger and V. Trappe, *Scientific Reports*, 2015, 5, 15520.

44. T. Gan, Y. Guan and Y. Zhang, *Journal of Materials Chemistry*, 2010, 20, 5937-5944.

45. J. F. Pollock and K. E. Healy, *Acta Biomater*, 2010, 6, 1307-1318.

46. A. Mellati, M. Valizadeh Kiamahalleh, S. Dai, J. Bi, B. Jin and H. Zhang, *Materials Science and Engineering: C*, 2016, 59, 509-513.

47. F. R. Maia, K. B. Fonseca, G. Rodrigues, P. L. Granja and C. C. Barrias, *Acta Biomaterialia*, 2014, 10, 3197-3208.

48. D. A. Balikov, S. W. Crowder, T. C. Boire, J. B. Lee, M. K. Gupta, A. M. Fenix, H. N. Lewis, C. M. Ambrose, P. A. Short, C. S. Kim, D. T. Burnette, M. A. Reilly, N. S. Murthy, M.-L. Kang, W. S. Kim and H.-J. Sung, *ACS Applied Materials & Interfaces*, 2017, 9, 22994-23006.

49. A. L. Barnes, P. G. Genever, S. Rimmer and M. C. Coles, *Biomacromolecules*, 2016, 17, 723-734.

50. Y. S. Pek, A. C. A. Wan and J. Y. Ying, *Biomaterials*, 2010, 31, 385-391.

51. M. M. Martino, M. Mochizuki, D. A. Rothenfluh, S. A. Rempel, J. A. Hubbell and T. H. Barker, *Biomaterials*, 2009, 30, 1089-1097.

52. C. Hildebrandt, H. Büth and H. Thielecke, *Tissue and Cell*, 2011, 43, 91-100.

53. S.-A. Oh, H.-Y. Lee, J. H. Lee, T.-H. Kim, J.-H. Jang, H.-W. Kim and I. Wall, *Tissue Engineering Part A*, 2011, 18, 1087-1100.

54. P. Occhetta, M. Centola, B. Tonnarelli, A. Redaelli, I. Martin and M. Rasponi, *Scientific Reports*, 2015, 5, 10288.

55. L. Zhao, G. Li, K.-M. Chan, Y. Wang and P.-F. Tang, *Calcified Tissue International*, 2009, 84, 56-64.

56. A. D. Theocharis, S. S. Skandalis, C. Gialeli and N. K. Karamanos, *Advanced Drug Delivery Reviews*, 2016, 97, 4-27.

57. J. Garcia, C. Mennan, H. S. McCarthy, S. Roberts, J. B. Richardson and K. T. Wright, *Stem Cells International*, 2016, 2016, 11.

58. S. Boeuf and W. Richter, *Stem Cell Research & Therapy*, 2010, 1, 31.

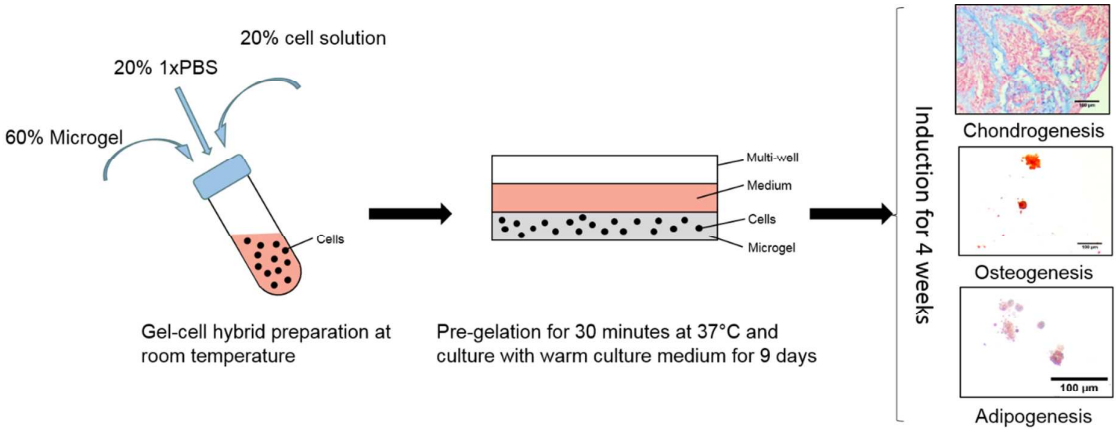

hMSCs derived from the normal donors were induced multi-lineage differentiation within the thermosensitive poly (N-isopropylacrylamide-co-acrylic acid) microgel-formed 3D constructs.